CHAPTER VII

ANTIBACTERIAL AND ANTICANCER ACTIVITIES OF THE rGO/CS/ METAL OXIDES (ZnO, CuO), METAL (Ag, Au) NANOCOMPOSITES

7.1 INTRODUCTION

The advancement of nanotechnology has led to a variety of nanomaterials that require investigations into their safety for human health and ecological purposes at the environmental and organism levels. Microorganisms such as bacteria and fungi are found in the environment such as water, soil, skin and air that can penetrate easily on various surfaces which leads to serious infectious diseases in both humans and animals. Almost seventeen thousand people die every year as a result of microbial infections [1]. Liver cancer is one among the major cause of death in economically developed countries. The increase in cancer mortality rates in many countries is due to population, aging and growth as well as an adoption of cancer associated lifestyle choices because of lack of physical activities, radiation, stress and environmental pollution. Despite the fact chemotherapy can significantly improve the quality of life of patients with liver cancer, but only a small amount of increase in survival rate is achieved due to poor bioavailability and drug resistance. Treatment to cancer still remains a challenging one to cure cancer completely [2].

To overcome this, many research groups have paid attention to develop various types of antimicrobial agents and novel nanomaterials to protect human life against the negative effects of microorganisms. Most importantly, targeting pathogenic bacteria with nanomaterials has received great attention. However, the traditional antibiotics lose their resistance to microorganisms since they develop their own resistance. Thereby, more attentions and efforts have been made to invent novel drugs to treat multidrug-resistant pathogens and cancer theraphy [3].

Graphene is a single atomic plane layer of the graphite structure. It is a two-dimensional planar and hexagonal array of carbon atoms. Each of these carbons are sp^2-hybridized and has four bonds, one σ bond with each of its three neighbours and one π-bond that is oriented out of the plane. It has a hexagonal pattern, forming

a honeycomb crystal lattice [4]. Graphene oxide (GO) is a promising functional nanobiomaterial that is widely applied in drug delivery, biosensing, photocatalysis, energy storage devices, electronics and biomedicine. The interactions between Graphene oxide and living organisms and their subsequent biological responses is one of the most active research fields in nanotoxicology [5]. The researchers developed various Graphene based nanocomposites by modifying the surface of graphene using biomolecules, polymers and inorganic materials to decrease the toxicity and to improve their antibacterial efficiency. The development of nanocomposites involving the combination of carbon nanomaterials with nobel metal or metal oxide nanoparticles will remarkably enhance their biological properties like antibacterial and anticancer activity [6]. Chitosan (CS), a basic polysaccharide natural bio copolymer of β [1,4]-glucosamine and N-acetyl-D glucosamine linked by glycosidic bonds and one of the most plentiful natural polymers on earth, is generally obtained through deacetylation of chitin [7]. Because of its unique properties like biodegreadation and biocompatablity, it is considered as a promising agent for applications in molecular separation, food packaging, biomedical, paper industry, artificial skin, bone substitutes, water treatment, electrochemical sensors, biosensors, etc., The functional groups of chitosan may be allowed to interact with other materials such as TiO_2, Cu_2O, CdS, zeolite, ZnO, Ag and Au for the applications in the field of removal of dyes, toxic organics, biosensors and antimicrobial agents [8].

This chapter deals with the antibacterial and anticancer studies of the synthesized metal (Au, Ag) / metal oxide (ZnO, CuO) nanoparticles decorated on the surface of chitosan blended reduced graphene oxide nanocomposites**.** The prepared nanocomposites are evaluated against gram-positive bacteria (Staphylococcus Aureus, Bacillus Subtilis) and gram-negative bacteria (Escherichia Coli, Klebsilla Pneumoniae) through disk diffusion method. The effect of anticancer is studied using the cytotoxicity effect. The cytotoxicity effect of the prepared nanocomposites is performed by MTT assay against liver cancer cell (HepG–2). The sample exhibits potential dose dependent cytotoxicity against HepG–2 (cancer cell line).

7.2 CLASSIFICATION OF BACTERIA

In 1800's **Danish scientist Hans Christian Gram** developed gram strain test to differentiate types of bacteria. In this method, bacteria which retain the crystal violet dye are called Gram-positive bacteria and in contrast bacteria that do not retain the violet dye are called Gram-negative bacteria as shown in the Figure 7.1[9].

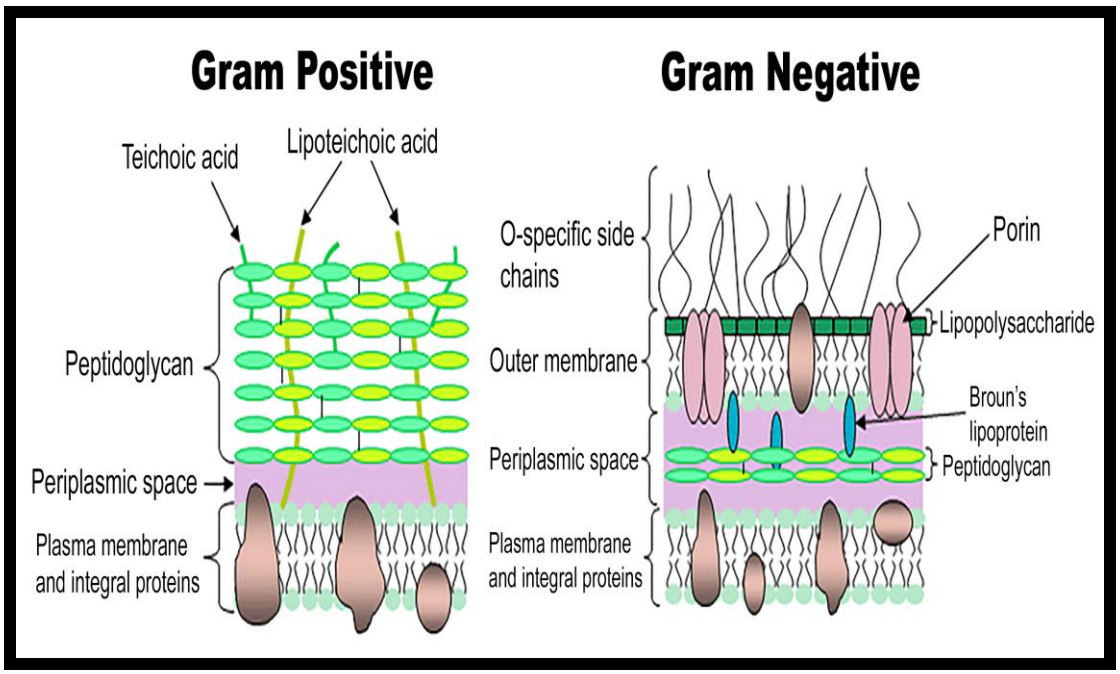

Figure 7.1 Shematic diagram of gram positve and gram negative bacteria

7.2.1 Gram positive bacteria

The bacteria that show purple stain during gram staining test are known as gram positive bacteria. It has a thick peptidoglycan layer and the thickness of the layer is around 20-30 nm which is responsible for retaining the strain. Porins are absent in gram positive bacteria. Only some species have flagella with two rings in the outer section. The surface layer is attached to the peptidoglycan layer. Nucleus is present in the centre part of the bacteria which is surrounded by cytoplasmic membrane, mitochondria, chromosomes, DNA and RNA [10].

7.2.2 Gram negative bacteria

The bacterium that shows pink stain during gram straining test are known as gram negative bacteria. It has both inner and outer cell membranes. It is bounded by

inner cell membrane and outer cell membrane with a thin layer of peptidoglycan in between these membranes. The inner cell membrane is called as cytoplasmic membrane. The outer cell membrane consists of lipopolysaccharides. Due to the lack of peptidoglycan layer gram negative bacteria do not retain stain. Porins are present in the outer cell membrane and four rings of flagella are also present in the outer membrane. The surface layer is directly attached to the outer membrane. It has nucleus in the centre part which is surrounded by cytoplasmic membrane, mitochondria, chromosomes, DNA and RNA [11].

7.3 FEATURES OF THE TEST ORGANISMS

The bacterial test organisms,

- ***Staphylococcus aureus***
- ***Bacillus subtilis***
- ***Escherchia coli***
- ***Klebsiella pneumonia*** are used in the present study.

7.3.1 Staphyloccocus aureus

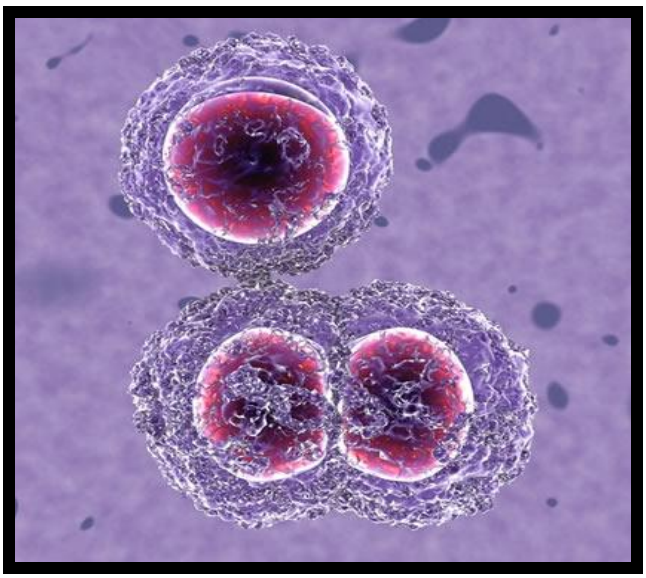

Figure 7.2 S.aureus

The name Staphylococcus arises from the Greek word staphyle, which means a bunch of grapes or kokkos, since the bacteria looks like a bunch of grapes on observing through the microscope as shown in the Figure 7.2. It is a Gram positive bacteria. They are approximately 0.5-1.5 μm in diameter and are non-moving, small round shaped or non-motile cocci. It is found in humans in the nose, groin, axillae, perineal area (males), mucous membranes, mouth, mammary glands, hair and the intestinal, genitourinary and upper respiratory tracts [12].

S aureus is an opportunistic infection which can cause a variety of serious diseases in humans. S,aureus is one of the most common causes for skin, soft-tissue and nosocomial infectiosn Scalded skin syndrome is caused by exfoliative toxins secreted on the epidermis and mostly affects neonates and young children [13].

7.3.2 Bacillus subtilis

Figure 7.3 Bacillus subtilis

Bacillus subtilis is a gram positive bacterium as shown in the Figure 7.3. At first it is named as vibrio subtilis by Christian Gottfried Ehrenberg in the year 1835and later it is renamed as Bacillus subtilis by Ferdinand Cohn in the year1872. It is also called as hay bacillus. They are rod-shaped and are about 4-10 μm length and 0.25–1.0 μm in diameter as shown in the Figure 7.3. It is found in soil and

the gastrointestinal tract of humans. It can contaminate the food, resulting in food poisoning [14].

7.3.3 Escherichia coli

Figure 7.4 Escherichia coli

Escherichia coli generally known as E.coli as shown in the Figure 7.4. It is a Gram-negative and is found in the lower intestine of warm blooded organisms. They are rod shaped and are about 2.0 μm length and 0.25-1.0 μm in diameter. The cell volume of the bacteria is about 0.6–0.7 μm^3. It lives in the digestive tracts of living organisms. Most E. coli strains are harmless, but some serotypes are pathogenic and can cause serious food poisoning in humans. There are many types of E. coli. Some strains of E. coli bacteria may cause severe disease like anemia or kidney failure, which leads to death [15].

Transmission of pathogenic E. coli often occurs via fecal–oral transmission. Common routes of transmission include: unhygienic food preparation, farm contamination due to manure fertilization, irrigation of crops with contaminated grey water or raw sewage and direct consumption of sewage-contaminated water. Food products associated with E. coli outbreaks include cucumber, raw ground beef, raw

seed sprouts or spinach, raw milk, unpasteurized juice, unpasteurized cheese and foods contaminated by infected food workers via fecal–oral route [16].

7.3.4 Klebsiella pneumonia

Figure 7.5 Klebsiella Pneumonia

Klebsiella Pneumonia is a gram – negative, non motile bacterium as shown in the Figure 7.5. The German bacteriologist **Edwin klebs** named the bacteria Klebsiella in the year 1834–1913. It is also known as Friedlander's bacillum, named in the honour of a German pathologist **Carl Friedlander**, who proposed that this bacterium was the etiological factor for the pneumonia seen especially in individuals such as people with chronic diseases or alcoholics. It is a rod shaped bacteria found in the flora of the mouth, skin and intestines. It naturally occurs in the soil [17].

The bacterium typically colonizes human mucosal surfaces of the oropharynx and gastrointestinal tract. The bacterium once enters the body; it can display high degrees of virulence and antibiotic resistance. It is found that if the bacteria are spread through the respiratory tract, it causes pneumonia or if the bacteria are spread through the blood it causes infection in the blood stream. The most common infection caused by klebsiella bacteria are bronchopneumonia and bronchitis. These infections have tendency to form disease like lung abscess, cavitation, empyema and pleural adhesions [18].

7.4 DETERMINATION OF ANTIBACTERIAL ACTIVITY

The purpose of the Antibacterial activity is to resist the growth of bacteria. The antibacterial activity of the prepared nano composites is screened against gram positive (Escherichia coli, Klebsiella pneumonia) and gram negative (Staphylococcus aureus, Bacillus subtilis) bacteria. The antibacterial activity is investigated by disc diffusion method.

7.5 MATERIALS AND METHODS

7.5.1 Reagents

Muller Hinton Agar Medium, nutrient broth, sterile forceps, sterile cotton swabs, std Ciprofloxacin disc and petri dish.

7.5.2 Preparation of inoculum

The inoculums for the experiment are prepared in fresh Nutrient broth from the preserved slant culture. The inoculums are standardized by adjusting the turbidity of the culture to that of 0.5 Mc Farland standards. The turbidity of the culture is adjusted by the addition of sterile saline or broth. .

7.5.3 Sterilization of forceps and cotton swabs

Cotton wool swab are sterilized by autoclaving or dry heat (only for wooden swabs) by packing the swabs in culture tubes, papers or tins etc. Forceps are sterilized by dipping in alcohol and burning off the alcohol using flame.

7.5.4 Experimental procedure

The antibacterial activity is investigated by disc diffusion method. It is also known as Kirby-bauer method. The standardized inoculums are inoculated in the Mueller-Hinton agar plate prepared earlier by using an aseptic technique at which the sterile swab is dipped in the inoculums and the excess liquid is gently removed by pressing and rotating the swab firmly against the side of the culture tube. The bacterial lawn is formed by streaking the on the surface of the Mueller-Hinton agar plate. The plate is swabbed in one direction by rotating the plate 3 times at an angle of 90° and it is then allowed to dry for 5 minutes in order to obtain uniform growth.

Each Petri dish is divided into 6 parts and in each part 100 µg of samples disc such as 0.002 M, 0.004 M, 0.006 M, 0.008 M, 0.01M disc (discs are soaked overnight in sample solution) and 10 µg of Std Ciprofloxacin disc are pressed gently on the disc using flame- sterilized forceps. Then Petri dishes are placed in the refrigerator at 4º C for diffusion and the plates are incubated at 37 º C for 24 hours. Then, the zone of inhibition is observed around and is measured using a scale [19-20].

7.6 RESULTS AND DISCUSSION

7.6.1 Antibacterial Activity of rGO/CS/ZnO nanocomposites against Gram Positive and Gram-Negative Bacteria

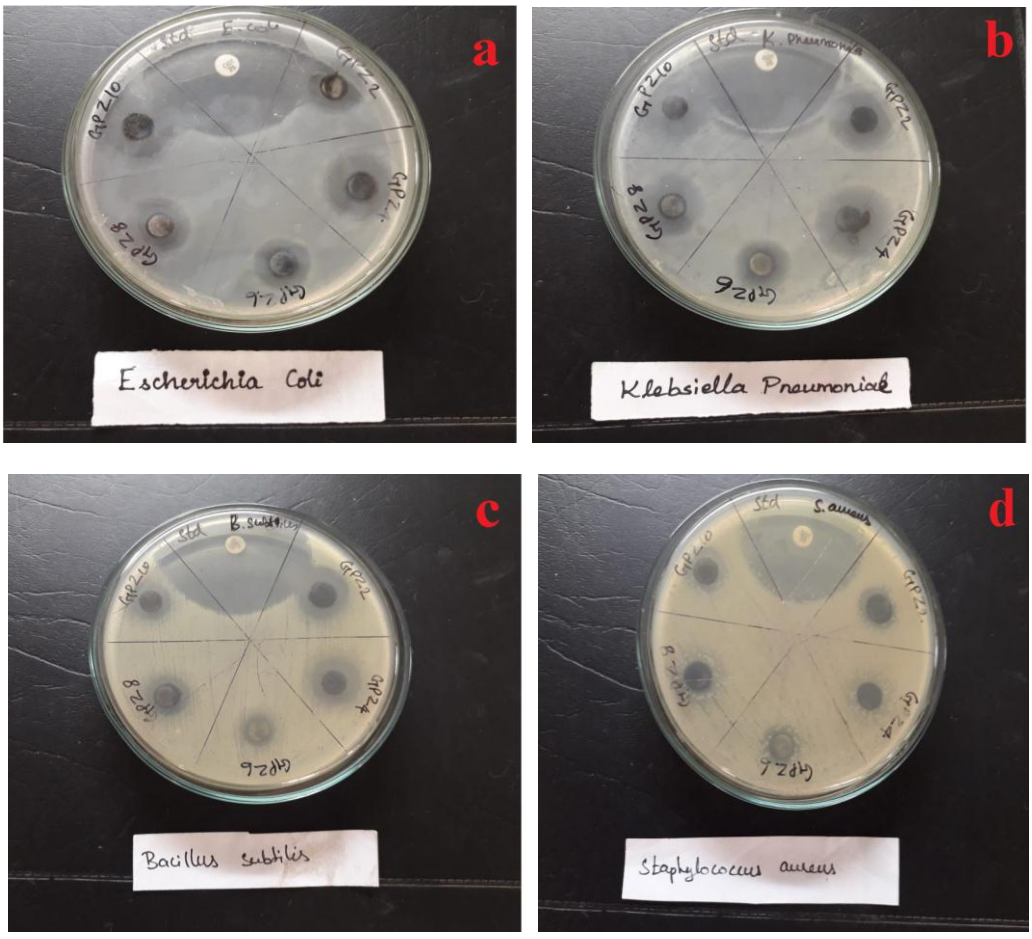

Figure.7.6 Antibacterial activity for various concentrations of rGO/CS/ZnO nanocomposites against Gram negative [(E.coli (a), K.pneumonia (b)] and Gram positive [(Bacillus subtilis (c), S.aureus (d)]

The antibacterial activity for various concentrations of rGO/CS/ZnO nanocomposites against Gram negative [(E.coli (a), K.pneumonia (b)] and Gram positive [(Bacillus subtilis (c), S.aureus (d)] is shown in the Figure 7.6 (a-d) . The gram positive and gram-negative organisms are placed in different petri dish and inoculated in the culture media. Each petri dish is divided into six parts at which 100 µg of different concentrations 0.002M, 0.004M, 0.006M, 0.008M and 0.01M of the prepared nanocomposites discs are added and the Zone of inhibition is measured after incubation. These zone of inhibition values for different concentrations of the rGO/CS/ZnO nanocomposites against Gram negative [(E.coli (a), K.pneumonia (b)] and Gram positive [(Bacillus subtilis (c), S.aureus (d)] is shown in the Figure 7.7 and its values are given in the Table 7.1. It is evident that the zone of inhibition increases gradually with increase in the concentration of Zinc oxide nanoparticles except for 0.006 M of Zinc oxide which may be due to the decrease in weight percentage of zinc oxide nanoparticles as evidenced from EDAX analysis.

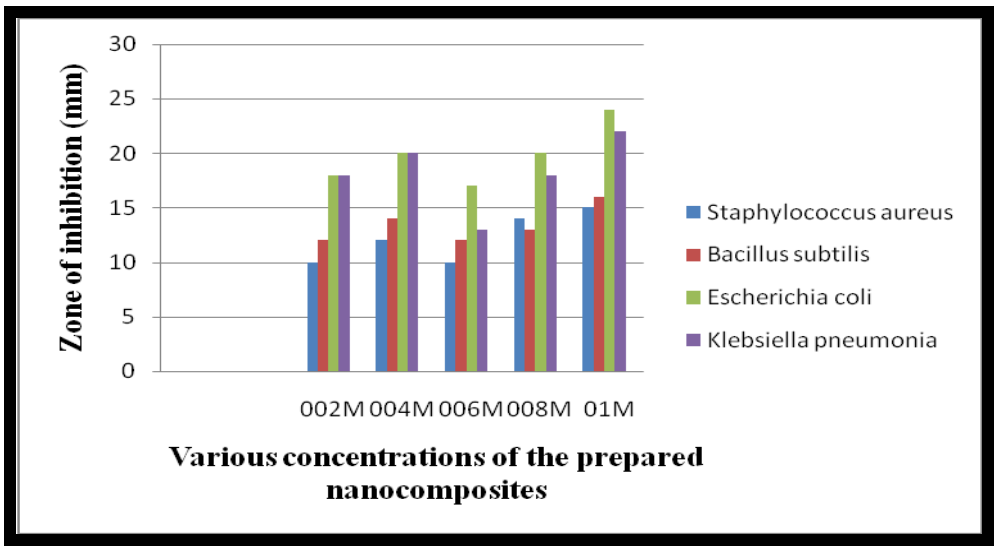

Figure 7.7 Graphical representation of zone of inhibition (mm) of various concentrations 0.002M, 0.004M, 0.006M, 0.008M and 0.01M of Zinc oxide nanorods incorporated on rGO/CS nanocomposites

Table 7.1 Antibacterial activity of various concentrations 0.002M, 0.004M, 0.006M, 0.008M and 0.01M of Zinc oxide nanorods incorporated on rGO/CS nanocomposites.

Antibacterial activity for Reduced graphene oxide/chitosan/Zinc nanocomposites					
Bacteria	Zone of Inhibition (mm)				
	0.002 M	0.004 M	0.006 M	0.008 M	0.01 M
S.aureaus	12	12	10	14	15
B.subtilis	12	16	13	17	20
E.coli	18	20	17	20	24
K.pneumoniae	18	20	13	18	22

It is further observed that the zone of inhibition for 0.008M and 0.01M of zinc oxide increases and may be due to the increase in number of particles on the surface of rGO/CS nanocomposites as evidenced from SEM analysis. Hence, the maximum zone of inhibiton is observed for 0.01M of rGO/CS/ZnO nanocomposites. These results shows that due to the symbiotic effect between zinc oxide, chitosan and reduced graphene oxide, the prepared nanocomposites exhibits excellent bactericidial activity against both gram positive and gram negative bacteria [21-22]. It is also observed that Gram negative bacteria shows excellent bactericidal activity compared to Gram positive bacteria. This may be due to Gram negative bacteria have thin peptidoglycan cell membranes compared to the Gram positive bacteria and it is easier for nanocomposites to penetrate into the bacteria cell membrane resulting in high bactericidial activity. The enhanced bactericidal activity is due to the generation of H_2O_2 molecules on the surface of ZnO which can penetrate through the cell membrane and inhibit the growth of bacteria [23-25].

7.6.2 Antibacterial Activity of rGO/CS/CuO nanocomposites against Gram Positive and Gram-Negative Bacteria

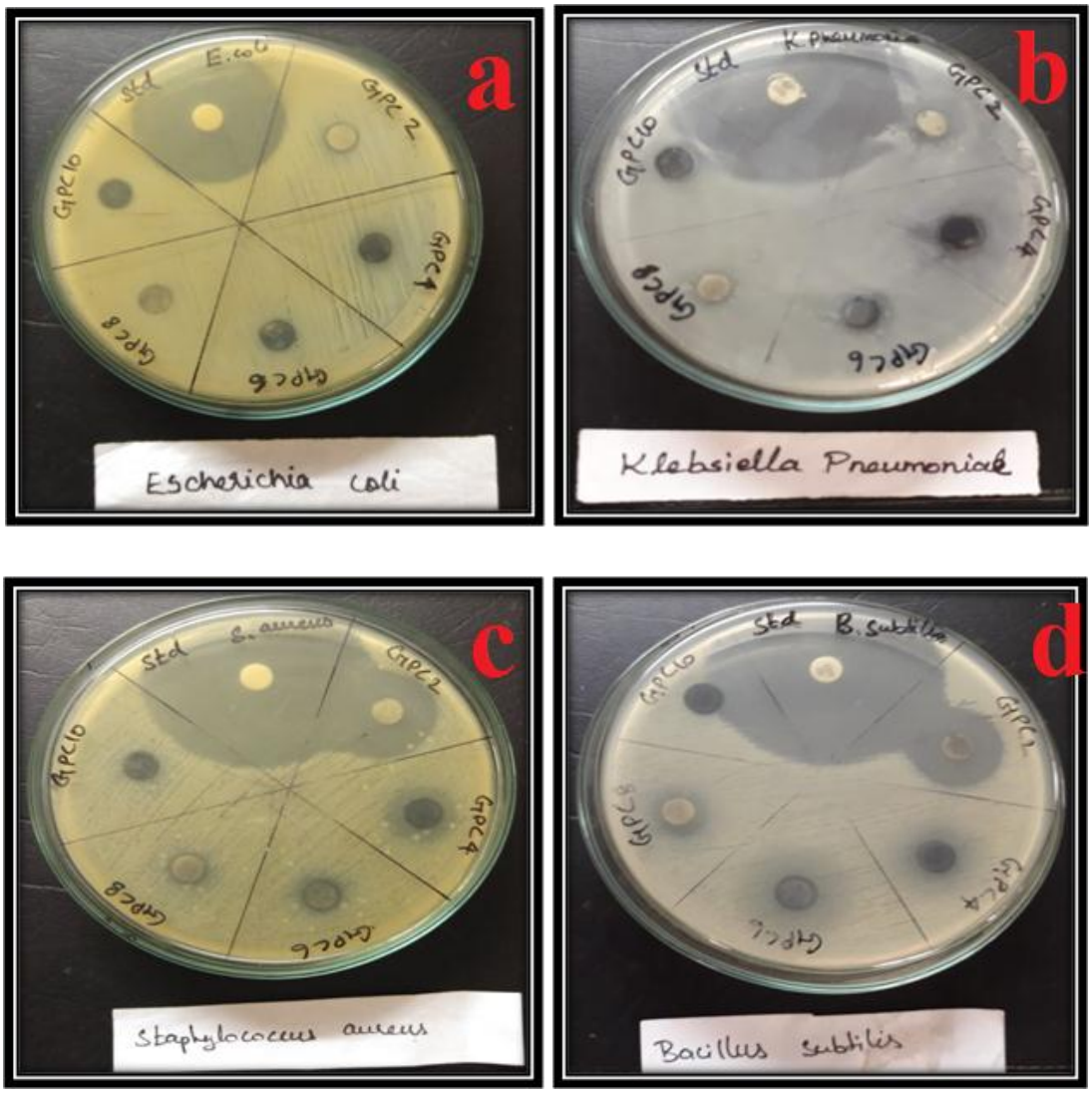

Figure 7.8 Antibacterial activity for various concentrations of rGO/CS/CuO nanocomposites against Gram negative [((a) E.coli (b) K.pneumonia] and Gram positive [(c) S.aureus (d) Bacillus subtilis]

The gram positive and gram-negative organisms are placed in various petri dish and inoculated in the culture media. Each petri dish is divided into six parts at which 100 µg of different concentrations 0.002 M, 0.004 M, 0.006 M, 0.008 M and 0.01 M of the prepared nanocomposites discs are added and the Zone of inhibition is measured after incubation. Figure7.8 (a-d) shows the antibacterial activity for

various concentrations of rGO/CS/CuO nanocomposites against Gram negative [(E.coli, K.pneumonia] and Gram positive [Bacillus subtilis, S.aureus]. It is observed from the Figure 7.8 (a-d) that both gram positive and gram negative bacteria exhibit excellent bactericidal activity against the prepared nanocomposites. The difference in bactericidal effect of both Gram-positive and Gram-negative bacteria may be due to the differences in their cell structure, metabolism and degree of contact of bacteria with the prepared nanocomposites [26-27]. It is further evident that Gram positive bacteria shows excellent bactericidal activity compared to Gram negative bacteria. This attributes that Cu^{2+} ions attaches to the negatively charged bacterial cell membrane by electrostatic attraction thus disruption in cell membrane. Thus the Cu^{2+} ions enters inside the bacteria, bind with other molecules leading to destruction in nuclei that result in the cell death [28-29].

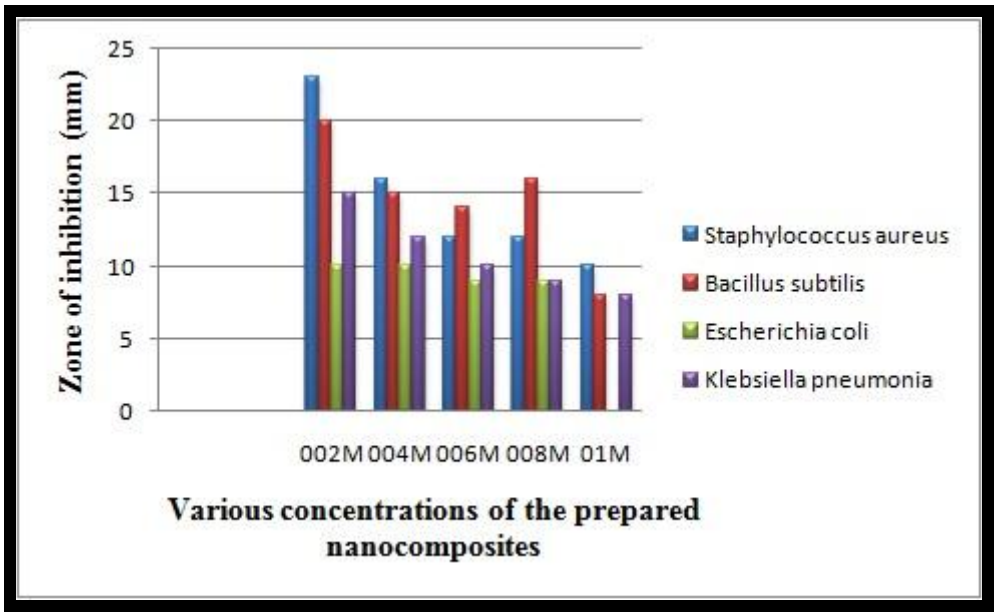

Figure 7.9 Graphical representation of zone of inhibition (mm) of various concentrations 0.002 M, 0.004 M, 0.006 M, 0.008 M and 0.01 M of copper oxide nanoparticles incorporated on rGO/CS nanocomposites

Table 7.2 Antibacterial activity of various concentrations 0.002M, 0.004M, 0.006M, 0.008M and 0.01M of copper oxide nanoparticles incorporated on rGO/CS nanocomposites.

Antibacterial activity for Reduced graphene oxide/chitosan/ copper oxide nanocomposites					
Bacteria	Zone of Inhibition (mm)				
	0.002 M	0.004 M	0.006 M	0.008 M	0.01 M
S.aureaus	23	16	12	12	10
B.subtilis	20	16	15	14	8
E.coli	10	10	9	9	-
K.neumoniae	15	12	10	9	8

The measured zone of inhibition values for different concentrations of the rGO/CS/CuO nanocomposites against Gram negative [(E.coli, K.pneumonia] and Gram positive [(Bacillus subtilis, S.aureus] is shown in the Figure 7.9 and its values are given in the Table 7.2. It is observed from the table that the measured zone of inhibition values decreases gradually with increase in the concentration of copper oxide nanoparticles. The maximum zone of inhibiton is observed for 0.002M of rGO/CS/CuO nanocomposites. This clearly indicates that with decrease in the particle size of prepared nanocomposites the bactericidal effect increases. Thus the zone of inhibition is inversely proportional to the particle size that may be due to the large surface to volume ratio of prepared nanocomposites.

7.6.3 Antibacterial Activity of rGO/CS/Ag nanocomposites against Gram Positive and Gram-Negative Bacteria

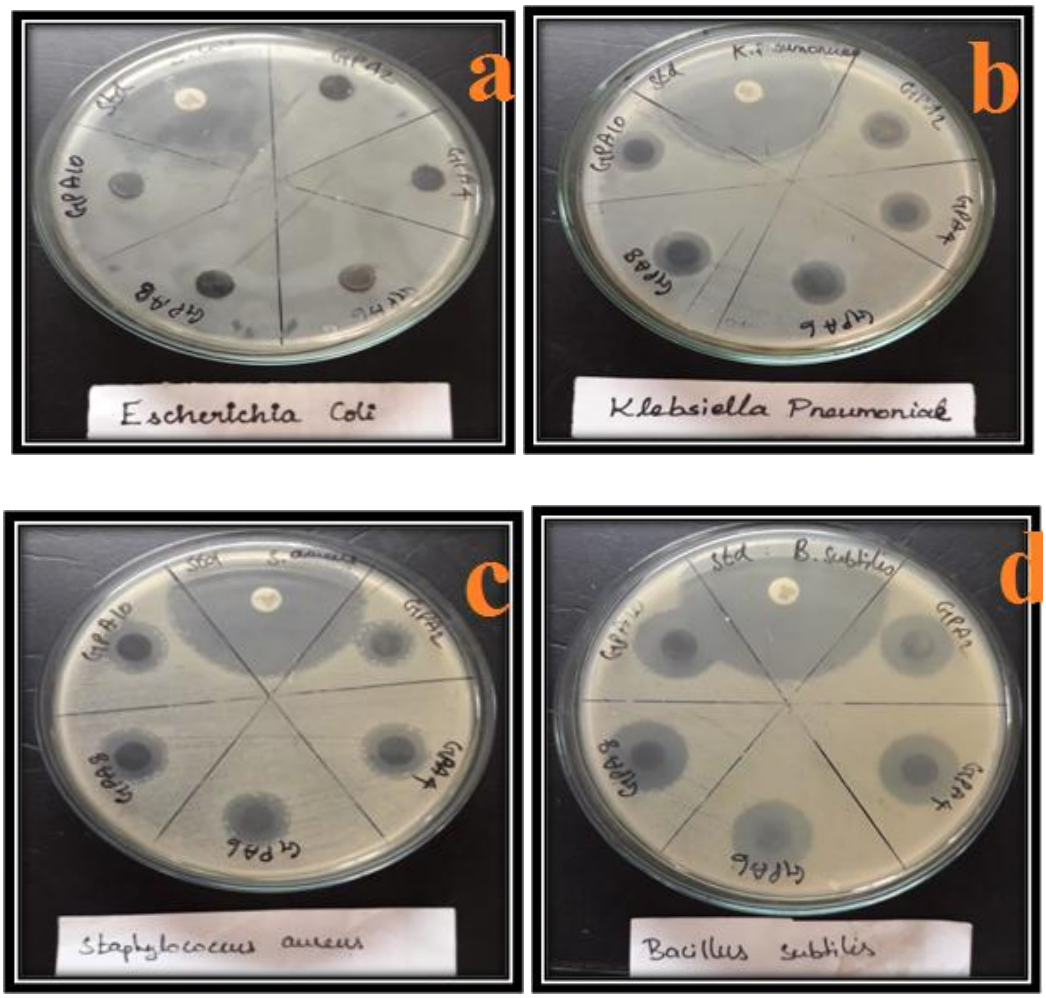

Figure 7.10 Antibacterial activity for various concentrations of rGO/CS/Ag nanocomposites against Gram negative [((a) E.coli (b) K.pneumonia] and Gram positive [(c) S.aureus (d) Bacillus subtilis]

The gram positive and gram-negative organisms are placed in various petri dish and inoculated in the culture media. Each petri dish is divided into six parts at which 100 µg of different concentrations 0.002M, 0.004M, 0.006M, 0.008M and 0.01M of the prepared nanocomposites discs are added and the Zone of inhibition is measured after incubation. Figure7.10 (a-d) shows the antibacterial activity for various concentrations of rGO/CS/Ag nanocomposites against Gram negative [(E.coli, K.pneumonia] and Gram positive [Bacillus subtilis, S.aureus]. It is

observed from the Figure 7.10 (a-d) that both Gram positive and Gram negative bacteria shows excellent bactericidal activity and the difference in bactericidal activity may be due to the difference in the cell membrane of the microgranisms. This attributes that the prepared rGO/CS/Ag nanocomposites interact with the bacertia cell membrane by electrostatic interaction leading to destruction in cell membrane [30]. The Ag^{+} ions penetrate into the bacteria and destroy all the membranes in the bacteria resulting in cell death. Moreover, rGO/CS/Ag nanocomposites generate reactive oxygen species (ROS) to inactive bacteria. Thus the ROS inhibits the bacterial growth which might result in bacterial death [31].

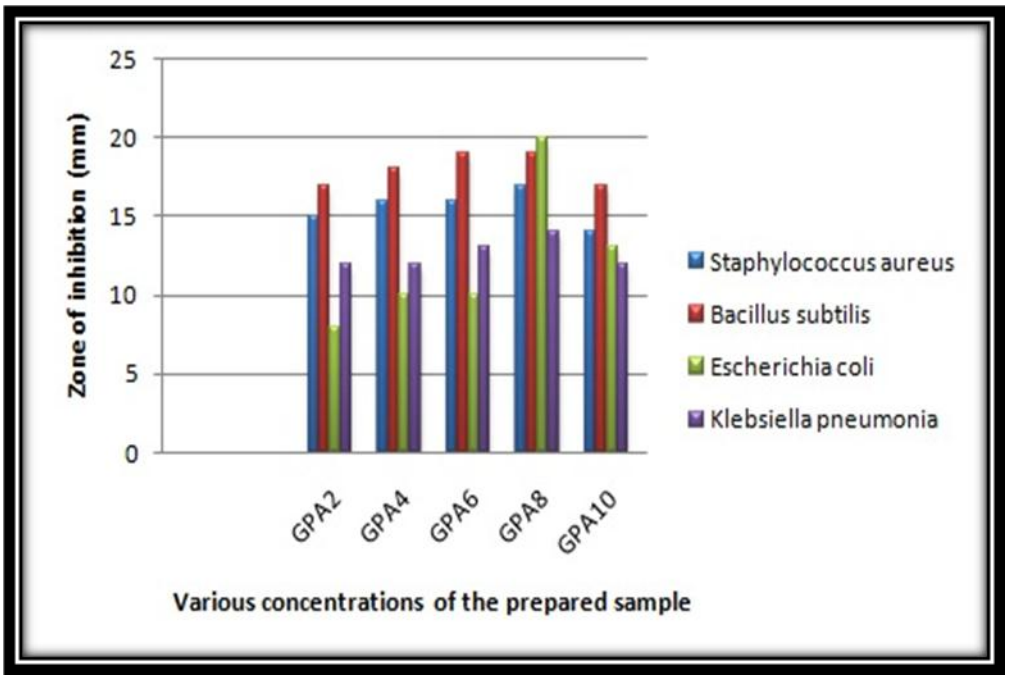

Figure 7.11 Graphical representation of zone of inhibition (mm) of various concentrations 0.002M, 0.004M, 0.006M, 0.008M and 0.01M of silver nanoparticles incorporated on rGO/CS nanocomposites

Table 7.3 Antibacterial activity of various concentrations 0.002M, 0.004M, 0.006M, 0.008M and 0.01M of silver nanoparticles incorporated on rGO/CS nanocomposites.

Antibacterial activity for Reduced graphene oxide/chitosan/Silver nanocomposites					
Bacteria	Zone of Inhibition (mm)				
	0.002 M	0.004 M	0.006 M	0.008 M	0.01 M
S.aureaus	15	16	16	17	11
B.subtilis	17	18	19	19	17
E.coli	08	10	10	20	13
K.neumoniae	12	12	13	14	12

The measured zone of inhibition values for different concentrations of the rGO/CS/Ag nanocomposites against Gram negative [(E.coli, K.pneumonia] and Gram positive [(Bacillus subtilis, S.aureus] is shown in the Figure 7.11 and its values are given in the Table 7.3. It is observed from the table that the measured zone of inhibition values increases gradually with increase in the concentration of silver nanoparticles from 0.002 M to 0.008 M and with further increase in the concentration of silver (0.01M) the zone of inhibition decreases. This decrease in zone of inhibition may be due to the aggregation of silver nanoparticles on the surface of rGO/CS nanocomposites as evidenced from SEM analysis as shown in the Figure 5.6. It is observed that for higher concentration of silver (0.01M), due to aggregation of silver nanoparticles, electrostatic interaction between prepared nanocomposites and microorganisms gets decreases thus resulting in poor bactericidal effect. The maximum zone of inhibiton is observed for 0.008 M of rGO/CS/Ag nanocomposites. Hence, the enhanced bactericidal activity is due to the large surface area of reduced graphene oxide/chitosan nanosheets with uniform dispersion of silver nanoparticles on its surface, which attributes the good electrostatic interaction prepared nanocomposites and microorganisms [32].

7.6.4 Antibacterial Activity of rGO/CS/Ag nanocomposites against Gram Positive and Gram-Negative Bacteria

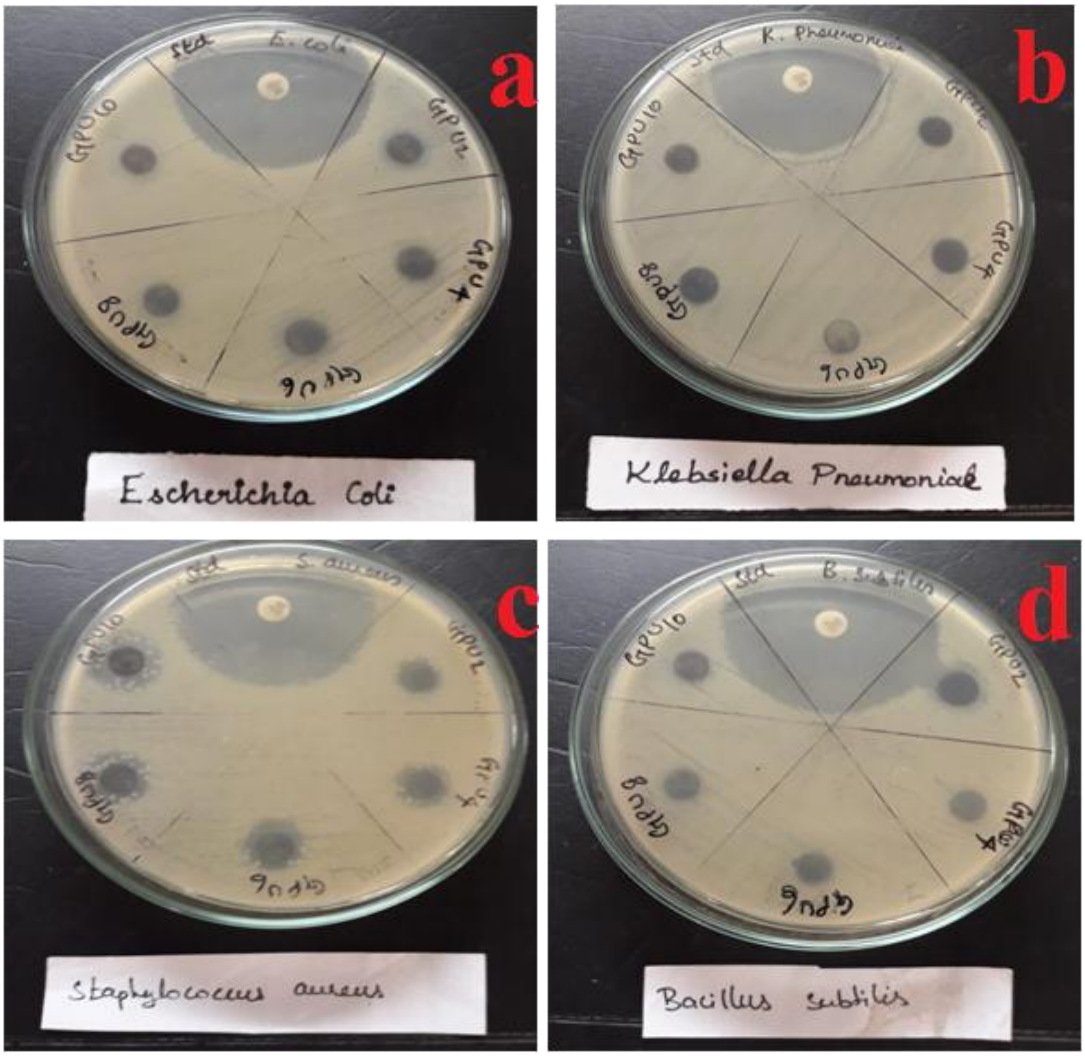

Figure 7.12 Antibacterial activity for various concentrations of rGO/CS/Au nanocomposites against Gram negative [((a) E.coli (b) K.pneumonia] and Gram positive [(c) S.aureus (d) Bacillus subtilis]

The microorganisms are inoculated in the culture media by placing it in various petri dishes. Each petri dish is divided into six parts at which 100 µg of different concentrations 0.002M, 0.004M, 0.006M, 0.008M and 0.01M of the prepared nanocomposites discs are added and the Zone of inhibition is measured after 24 hours of incubation. Figure7.12 (a-d) shows the antibacterial activity for various concentrations of rGO/CS/Au nanocomposites against Gram negative [(E.coli, K.pneumonia] and Gram positive [Bacillus subtilis, S.aureus]. It is

observed from Figue 7.12 (a-d) that Gram negative bacteria exhibits high bactericidal activity compared to Gram positive bacteria. However, Gram negative bacteria have thin peptidoglycan layer and the prepared rGO/CS/Au nanocomposites penetrates easily into the bacteria. Consequently the rGO/CS/Au nanocomposites releases ROS like H_2O^2, O_2^- that destructs the cytoplasm, nuclei of the bacteria and even damages DNA which leads to bacterial death [33].

The measured zone of inhibition values for different concentrations of the rGO/CS/Au nanocomposites against Gram negative [(E.coli, K.pneumonia] and Gram positive [(Bacillus subtilis, S.aureus] is shown in the Figure 7.13 and its values are given in the Table 7.4. It is observed from the table that the measured zone of inhibition values increases gradually with increase in the concentration of gold nanoparticles from 0.002 M to 0.01 M of gold nanoparticles. Since ROS is one of the major cause for bactericidal effect, due to the large surface area of prepared rGO/CS/Au nanocomposites the concentration of O_2^- increases leading to oxidative imbalance in bacteria, Au^+ ions attacksthe superoxide ions in the peptide linkages, resulting in destruction of the proteins. As a result of these the bacteria gets collapsed resulting in cell damage [34].

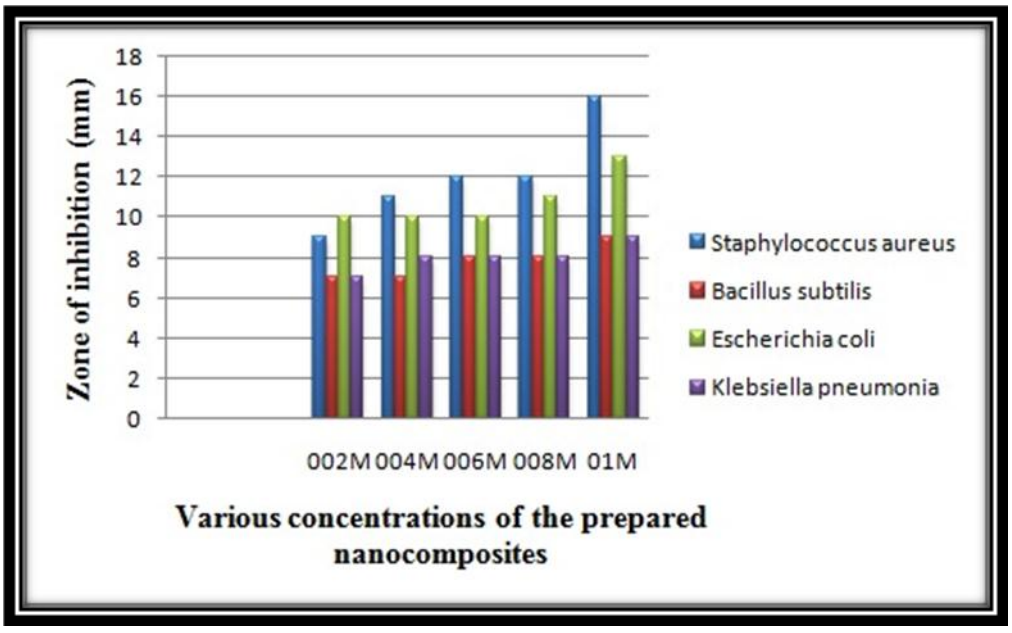

Figure 7.13 Graphical representation of zone of inhibition (mm) of various concentrations 0.002 M, 0.004 M, 0.006 M, 0.008 M and 0.01 M of gold nanoparticles incorporated on rGO/CS nanocomposites

Table 7.4 Antibacterial activity of various concentrations 0.002M, 0.004M, 0.006M, 0.008M and 0.01M of gold nanoparticles incorporated on rGO/CS nanocomposites.

Antibacterial activity for Reduced graphene oxide/chitosan/Gold nanocomposites					
Bacteria	Zone of Inhibition (mm)				
	0.002 M	0.004 M	0.006 M	0.008 M	0.01 M
S.aureaus	9	11	12	12	16
B.subtilis	7	7	8	8	9
E.coli	10	10	10	11	13
K.neumoniae	7	7	8	8	9

7.7 DETERMINATION OF ANTICANCER ACTIVITY

From the result of Antibacterial activity, highy inhibited nanocomposites are taken for anticancer studies. The Anticancer activity of the prepared nanocomposites is tested using cytotoxic assay. The cytotoxicity of the prepared nanocomposites against liver cancer cell line (HepG2) is determined by MTT.

7.7.1 Materials

3-(4, 5- dimethylthiazol-2yl)-2,5- diphenyl- tetrazolium bromide, a yellow tetrazole (MTT), phosphate buffered saline (PBS), Dimethyl sulphoxide (DMSO), Dulbeco’s modified eagle medium (DMEM), fetal bovine serum (FBS), 96-well microtiter plate are obtained from sigma Aldrich chemical.

7.7.2 Cell line culture

HepG2 cancer cell lines are obtained from National centre for cell sciences pune (NCCS). The HepG2 cancer cells are cultured in Dulbecco's Modified Eagle's

Medium (DMEM) supplemented with 10% Fetal Bovine Serum (FBS), 20µg/ml penicillin and 100 µg/ml streptomycin. The cells are incubated at 37 °C with an atmosphere of 5% CO_2 in 96- well plates.

7.7.3 Cytotoxicity assay

The anticancer activity of the prepared nanocomposites on HepG2 cells are determined by the MTT assay. Human hepatocarcinoma (HepG–2) cell lines are cultured under standard cell culture conditions. HepG-2 cell lines are seeded in 96 well plates at the density of $1x10^5$ cells per well and kept in an incubator at $37^{\circ}C$ for 24 hours. The cells are treated with various concentrations (25, 50, 75, 100 and 125 µg/ml) of the prepared nanocomposites by serial dilution method. The cells are then incubated at 37 °C in a humidified incubator with 5 % CO_2, 75 % relative humidity for 24 hours. After 48 hours of incubation, 10µl of MTT is added to each well and incubated for 4 hours at 37°C. The medium with MTT is removed and the formed formazan crystals are solubilized in 100µl of DMSO solution. After the medium is aspirated Dimethyl sulfoxide (DMSO) is added into the cells and its absorbance is measured at 570 nm using a photometer [35-36]. Cytotoxicity and Cell viability of the samples are calculated using the formula

$$\text{Cytotoxicity} = [(\text{Control} - \text{Treated})/\text{Control}] \times 100$$

$$\text{Cell Viability} = (\text{Treated}/\text{Control}) \times 100$$

7.8 RESULTS AND DISCUSSION

7.8.1 Anticancer Activity of rGO/CS/ZnOnanocomposites

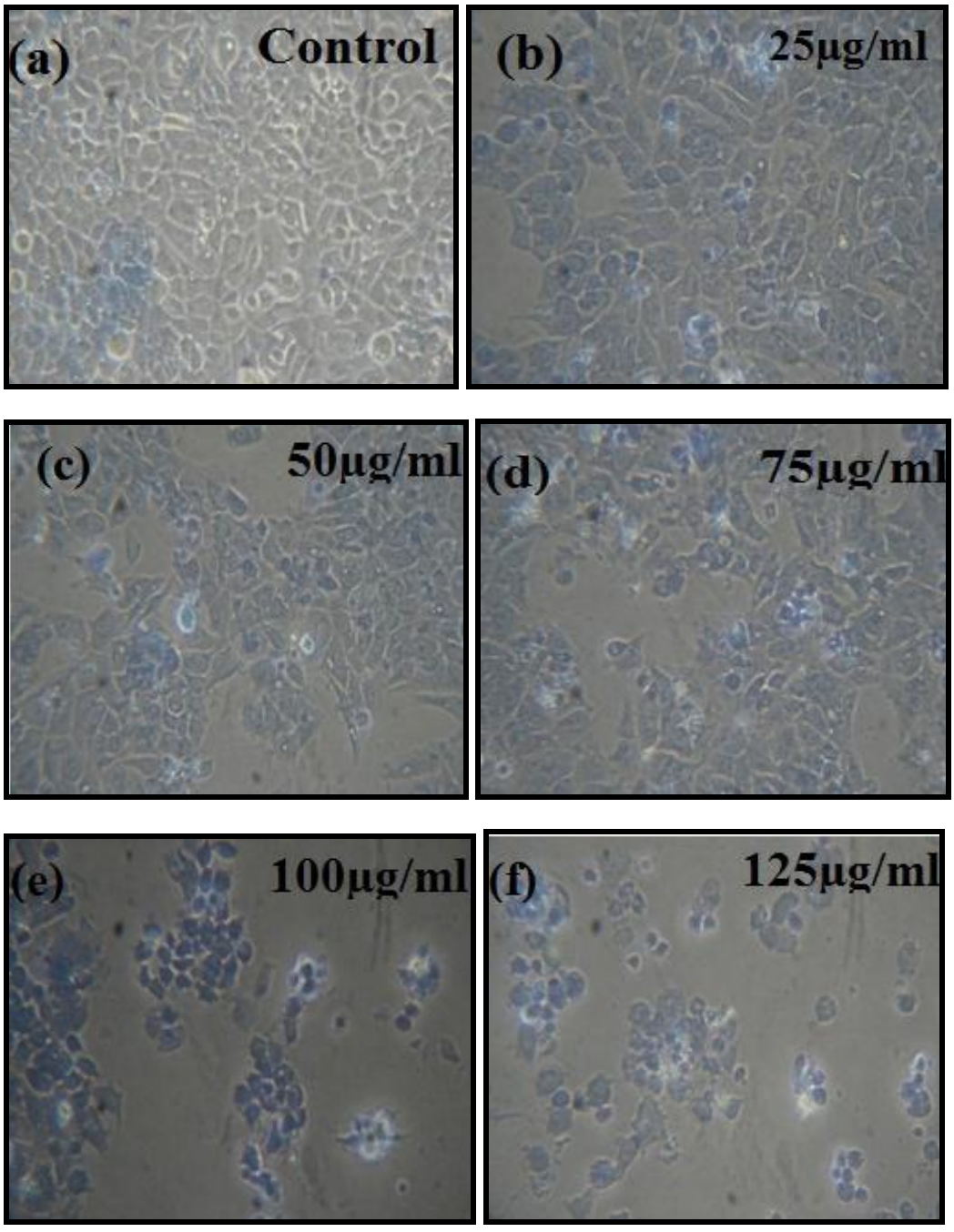

Figure 7.14 (a-e) Morphological assessment of anticancer activity for various concentrations of 0.01M of zinc oxide nanoparticles decorated on the surface of rGO/CS nanocomposite against HepG-2 cell line

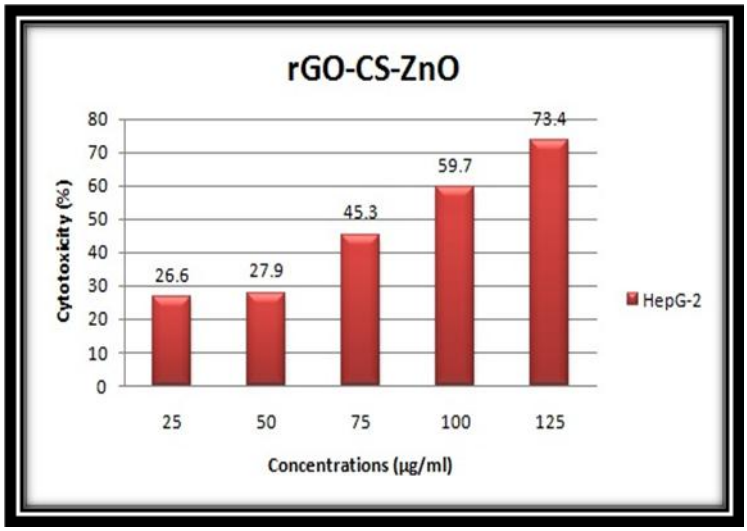

Figure 7.15 Cytotoxic effect of various concentrations of 0.01M of ZnO nanorods decorated on the surface of rGO/CS nanocomposite against HepG-2 cell line

The cytotoxic activity of the prepared nanocomposite in suppressing the growth of HepG-2 cell line is assessed using MTT assay. Figure 7.14 shows the morphological assessment of anticancer activity for various concentrations (25 µg/ml, 50 µg/ml, 75 µg/ml, 100 µg/ml and 125 µg/ml) of 0.01 M of rGO/CS/ZnO nanocomposites against HepG-2 cell line. The morphology depicts that on treating the rGO/CS/ZnO nanocomposites against HepG-2 cell line, the cell gets shrinked and density of the cells have been reduced on increasing the concentration of the sample.

Figure 7.15 shows the cytotoxicity graph for various concentrations of 0.01M of rGO/CS/ZnO nanocomposites against the HepG-2 cancer cell line using dose dependent approach. It is observed from the Figure 7.15 that the effective cytotoxicity rate is 75%, which is observed for 125µg/ml. The cytotoxicity rate against HepG-2 cell line increases with an increase in the concentration of the sample.

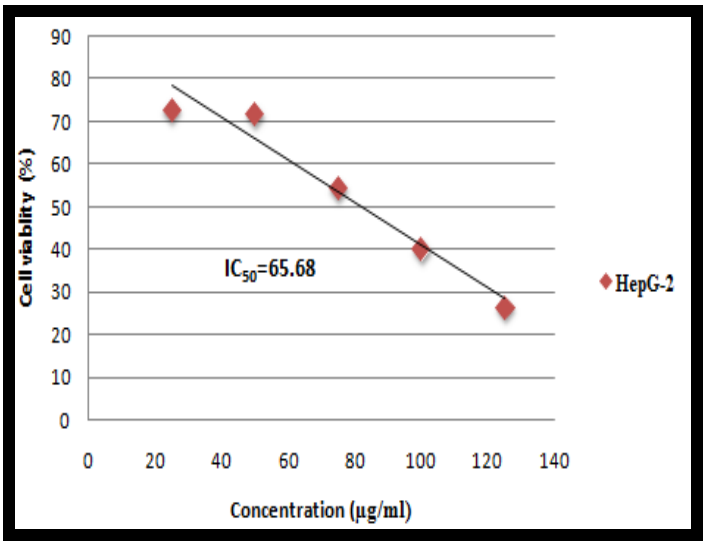

Figure 7.16 Percentage of viability vs various concentration of 0.01M of ZnO nanorods decorated on the surface of rGO/CS nanocomposite against HepG-2 cell line

Figure 7.16 shows the cell viability curve for 0.01M of rGO/CS/ZnO nanocomposite against the same cell line. Cell viability is decreased to 73%, 72%, 54%, 40%, and 26% for various concentrations of 25, 50, 75, 100 and 125 µg/ml of 0.01M of rGO/CS/ZnO nanocomposites respectively as depicted in the Figure 7.14 (b). The decrease in cell viability is about 26% for125 µg/ml.

The inhibitory concentration IC (50) of the prepared rGO/CS/ZnO nanocomposites against HepG-2 cell line is found to be about 34.6 µg/ml. Thus the effective cytotoxicity of the nanocomposite is due to the interaction between positively charged ZnO nanorods and the negatively charged surface of cancer cell line, which enhances the antioxidant properties towards the HepG-2 cell line [37].

7.8.2 Anticancer Activity of rGO/CS/CuOnanocomposites

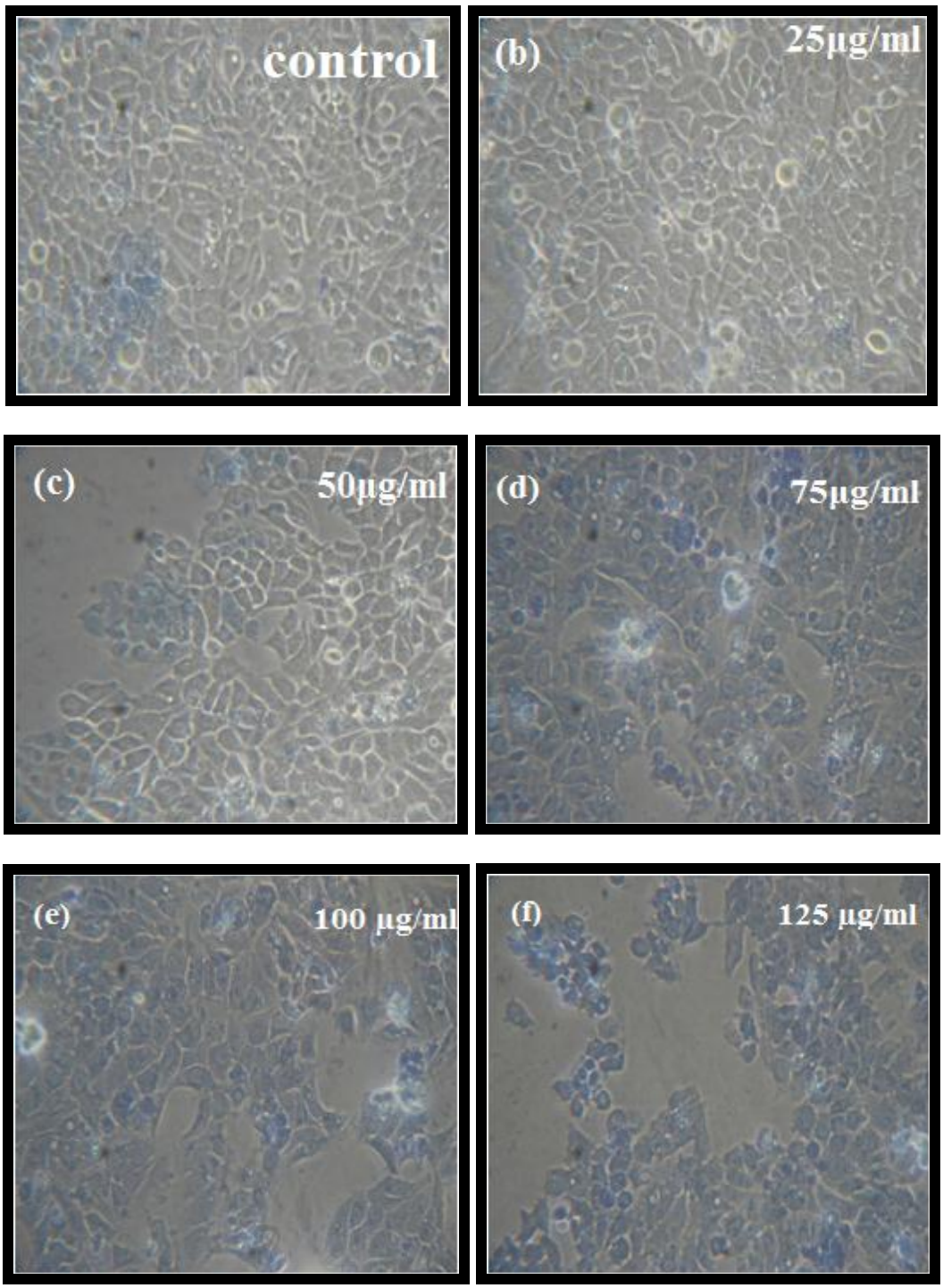

Figure 7.17 (a-e) Morphological assessment of anticancer activity for various concentrations of 0.002M of copper oxide nanoparticles decorated on the surface of rGO/CS nanocomposite against HepG-2 cell line

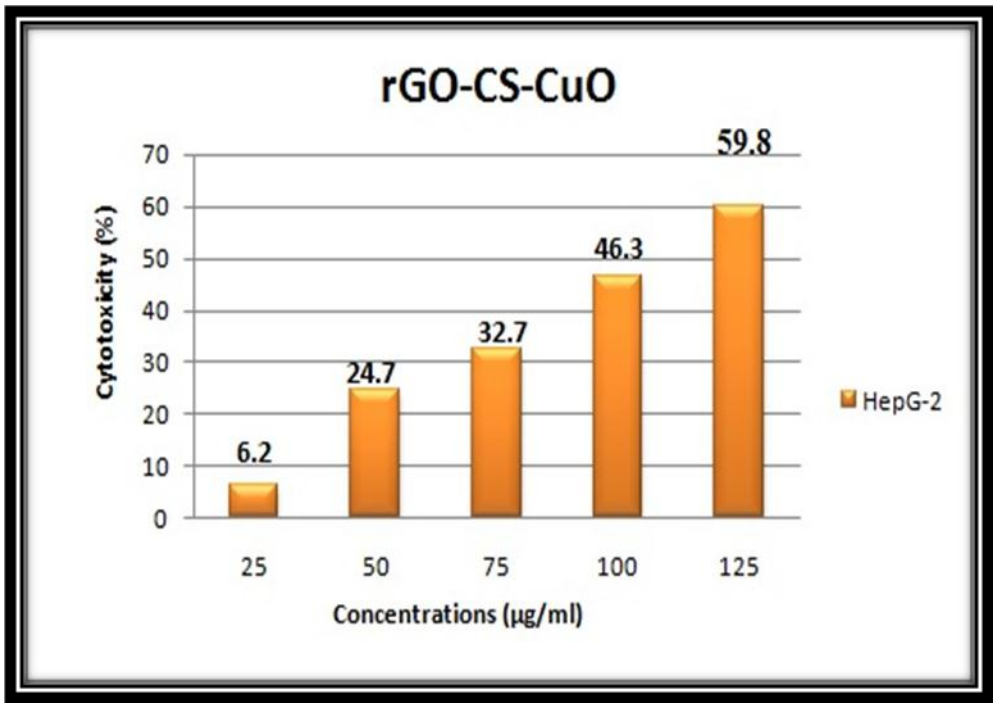

Figure 7.18 cytotoxicity for 0.002 M of CuO nanocomposites decorated on the surface of rGO/CS nanocomposite against HepG-2 cell line

The cytotoxic activity of the prepared nanocomposite in suppressing the growth of HepG-2 cell line is assessed using MTT assay. Figure 7.17 shows the morphology of HepG-2 cell line on treating with various concentrations (25 µg/ml, 50 µg/ml, 75 µg/ml, 100 µg/ml and 125 µg/ml) of 0.002 M of rGO/CS/CuO nanocomposites. The morphology shows the apoptotic changes like cell shrinkage, decrese in cell density compared to control.

Figure 7.18 shows the cytotoxicity graph for various concentrations (25 µg/ml, 50 µg/ml, 75 µg/ml, 100 µg/ml and 125 µg/ml) of 0.002 M of rGO/CS/CuO nanocomposites against the HepG-2 cancer cell line using dose dependent approach. The Figure depicts that the cytotoxicity percentage increases from 6.2%, 24.7%, 32.7%, 46.3% and 59.8% for 25 µg/ml, 50 µg/ml, 75 µg/ml, 100 µg/ml and 125 µg/ml respectively. The cytotoxicity rate against HepG-2 cell line increases with an increase in the concentration of the sample. The highest cytotoxicity rate is 59.8% for 125 µg/ml [38].

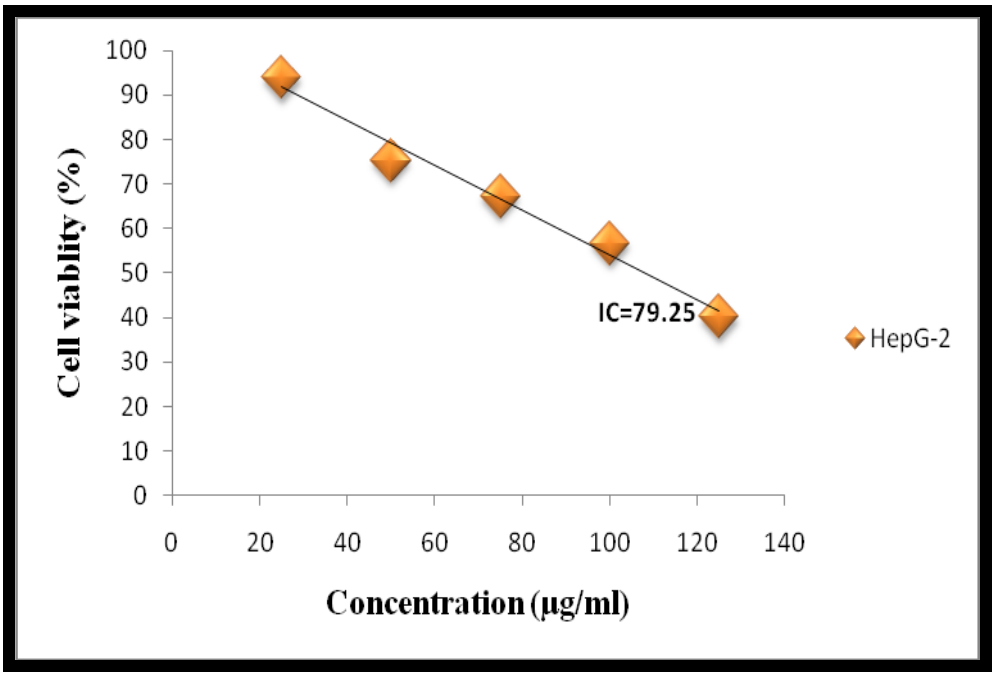

Figure 7.19 Percentage of viability vs various concentration of 0.002 M of CuO nanocomposites decorated on the surface of rGO/CS nanocomposite against HepG-2 cell line

Figure 7.19 shows the cell viability curve for various concentrations (25 µg/ml, 50 µg/ml, 75 µg/ml, 100 µg/ml and 125 µg/ml) of 0.002 M of rGO/CS/CuO nanocomposites against the same cell line. Cell viability is decreased to 93.8%, 75.3%, 67.3%, 56.7%, and 40.2% for various concentrations of 25, 50, 75, 100 and 125 µg/ml of 0.01M of rGO/CS/ZnO nanocomposites respectively as depicted in the Figure 7.18. The decrease in cell viability is about 26% for125 µg/ml.The inhibitory concentration IC (50) of the prepared nanocomposites against HepG-2 cell line is found to be about 21.05 µg/ml.

7.8.3 Anticancer Activity of rGO/CS/Ag nanocomposites

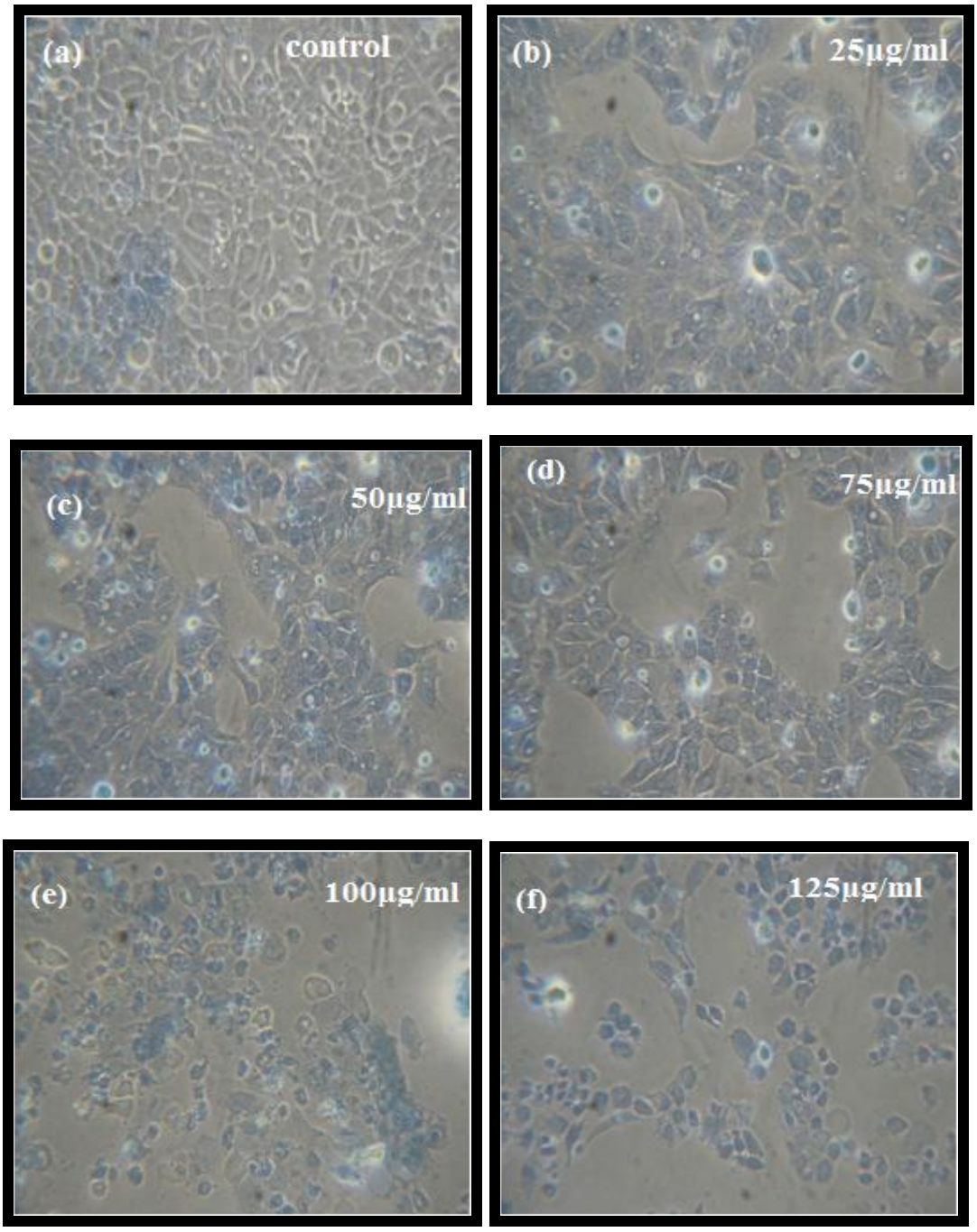

Figure 7.20 (a-e) Morphological assessment of anticancer activity for various concentrations of 0.008 M of Ag nanoparticles decorated on the surface of rGO/CS nanocomposite against HepG-2 cell line

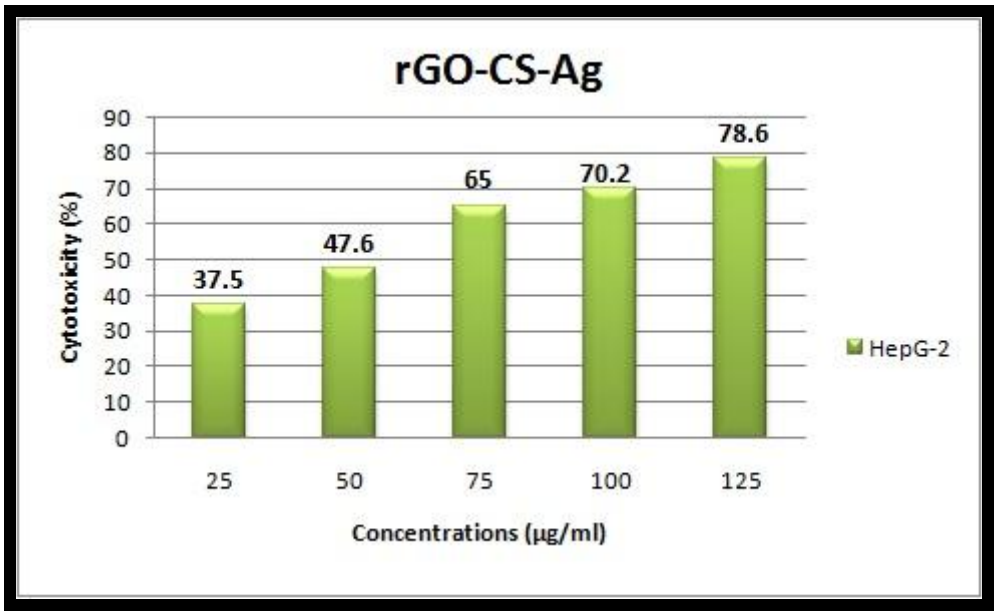

Figure 7.21 cytotoxicity for 0.002 M of Ag nanocomposites decorated on the surface of rGO/CS nanocomposite against HepG-2 cell line

The in vitro cytotoxicity of the prepared nanocomposite against HepG-2 cell line is investigated using MTT assay. Figure 7.20 shows the morphology of HepG-2 cell line on treating with various concentrations (25 µg/ml, 50 µg/ml, 75 µg/ml, 100 µg/ml and 125 µg/ml) of 0.008 M of rGO/CS/Ag nanocomposites. After 24 hours of incubation the morphology of the cancer line shows that the amount of apoptotic cells significantly increases on treating with rGO/CS/Ag nanocomposites.

Figure 7.21 shows the cytotoxicity graph for various concentrations (25 µg/ml, 50 µg/ml, 75 µg/ml, 100 µg/ml and 125 µg/ml) of 0.008 M of rGO/CS/Ag nanocomposites against the HepG-2 cancer cell line using dose dependent approach. The Figure depicts that the cytotoxicity percentage increases from 37.5%, 47.6%, 65%, 70.2% and 78.6% for 25 µg/ml, 50 µg/ml, 75 µg/ml, 100 µg/ml and 125 µg/ml respectively. The cytotoxicity rate against HepG-2 cell line increases with an increase in the concentration of the sample. The highest cytotoxicity rate is 78.6% for125 µg/ml. Thus the antiproliferative activity of the prepared nanocomposite is due to the induction of reactive oxygen species (ROS) which inhibits the cell growth and leads to apoptotis or cell death [39].

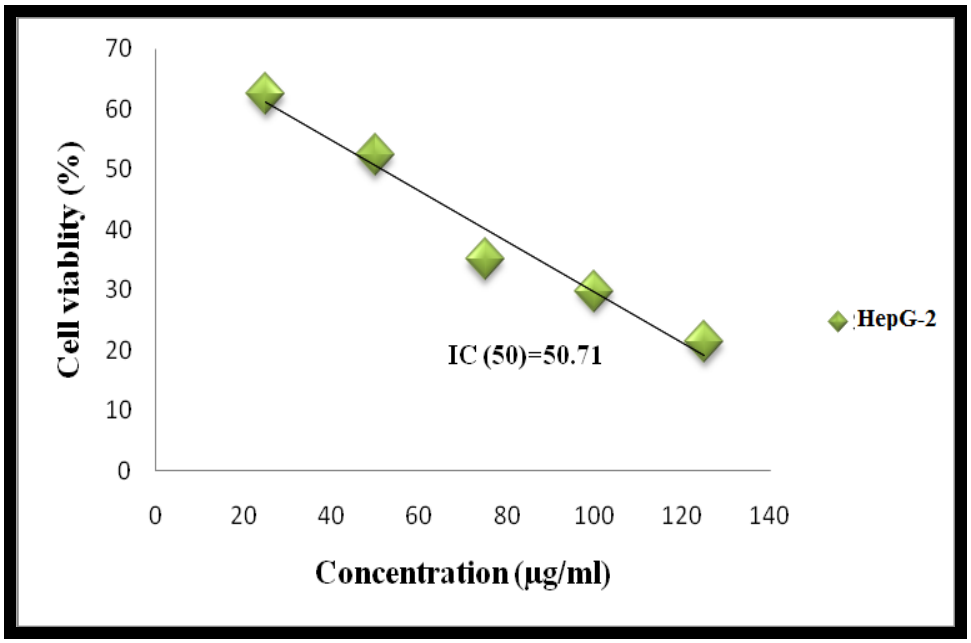

Figure 7.22 Percentage of viability vs various concentration of 0.008 M of Ag nanocomposites decorated on the surface of rGO/CS nanocomposite against HepG-2 cell line

Figure 7.22 shows the cell viability curve for various concentrations (25 µg/ml, 50 µg/ml, 75 µg/ml, 100 µg/ml and 125 µg/ml) of 0.002 M of rGO/CS/CuO nanocomposites against the same cell line. The percentage of cell viability is decreased to 62.5%, 52.4%, 35%, 29.8%, and 21.4% for various concentrations of 25, 50, 75, 100 and 125 µg/ml of 0.008M of rGO/CS/Ag nanocomposites respectively as depicted in the Figure 7.21. The decrease in cell viability is about 21.4 % for125 µg/ml. The inhibitory concentration IC (50) of the prepared nanocomposites against HepG-2 cell line is found to be about 19.29 µg/ml. These results indicate that the prepared nanocomposites show potent anticancer activity against HepG-2 cell line.

7.8.4 Anticancer Activity of rGO/CS/Au nanocomposites

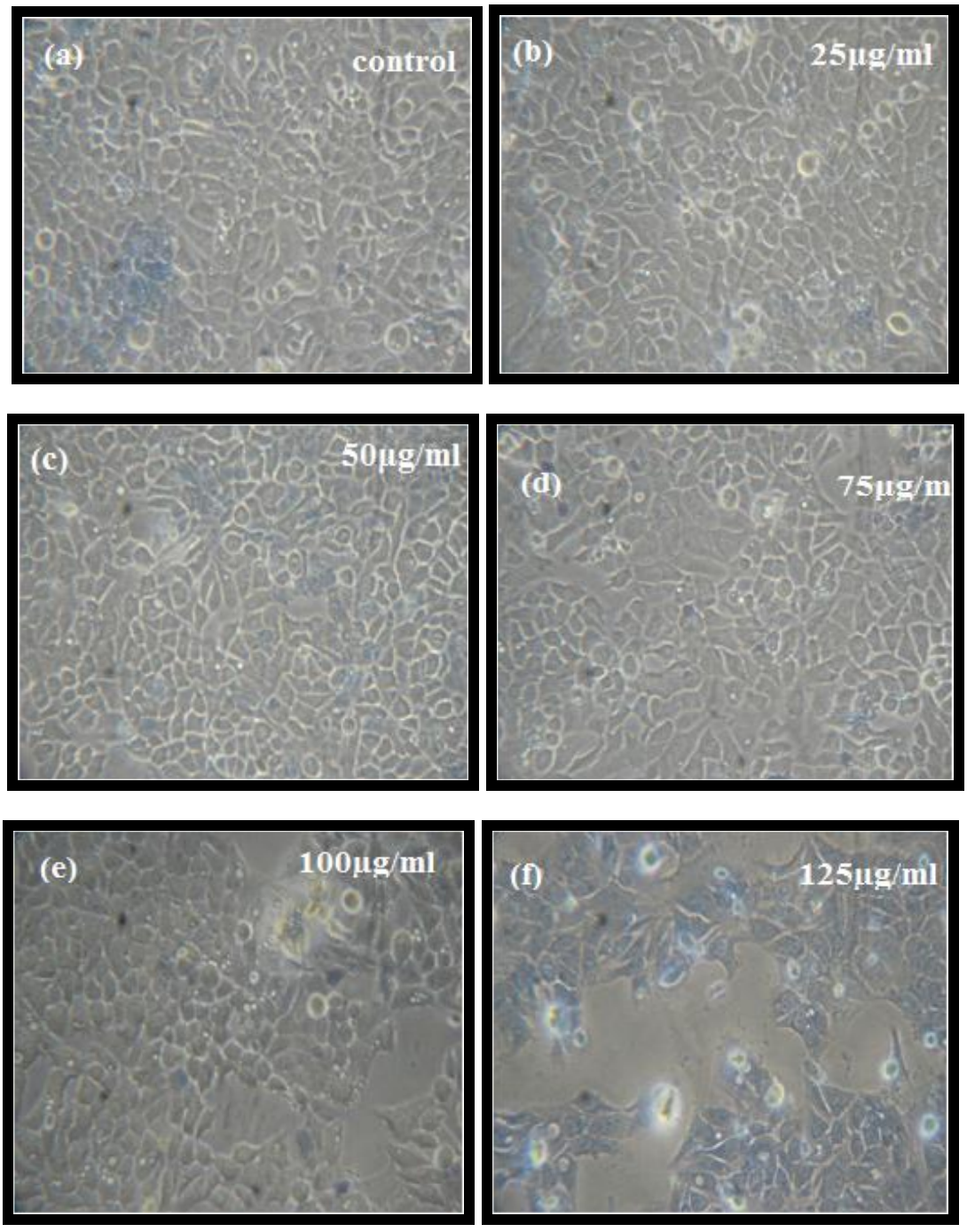

Figure 7.23 (a-e) Morphological assessment of anticancer activity for various concentrations of 0.01 M of Au nanoparticles decorated on the surface of rGO/CS nanocomposite against HepG-2 cell line

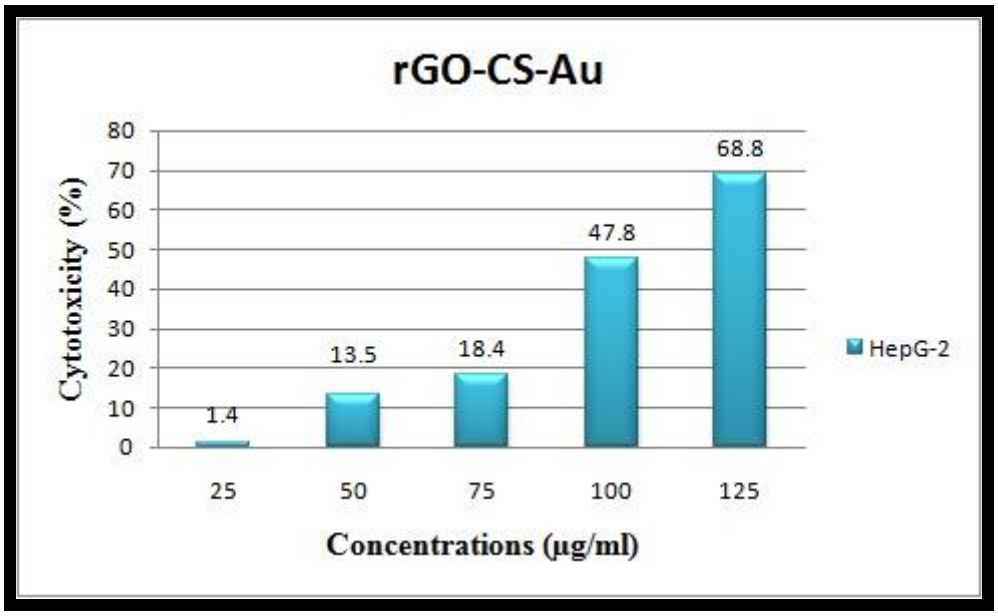

Figure 7.24 Cytotoxicity effect for various concentrations of 0.01 M of Au nanocomposites decorated on the surface of rGO/CS nanocomposite against HepG-2 cell line

The in vitro cytotoxicity of the prepared rGO/CS/Au nanocomposite against HepG-2 cell line is investigated using MTT assay. Figure 7.23 shows the morphology of HepG-2 cell line on treating with various concentrations (25 µg/ml, 50 µg/ml, 75 µg/ml, 100 µg/ml and 125 µg/ml) of 0.01 M of rGO/CS/Au nanocomposites. After treating the cancer cell line with 2 various concentrations (25 µg/ml, 50 µg/ml, 75 µg/ml, 100 µg/ml and 125 µg/ml) of 0.008 M of rGO/CS/Au nanocomposites the selected cell shows decrease in cell density compared to non treated control cell line.

Figure 7.24 shows the cytotoxicity graph for various concentrations (25 µg/ml, 50 µg/ml, 75 µg/ml, 100 µg/ml and 125 µg/ml) of 0.01 M of rGO/CS/Au nanocomposites against the HepG-2 cancer cell line using dose dependent approach. The Figure depicts that the cytotoxicity percentage increases from 1.4%, 13.5%, 18.4%, 47.8% and 68.8% for 25µg/ml, 50µg/ml, 75µg/ml, 100µg/ml and 125µg/ml respectively. The antiproliferative activity against HepG-2 cell line increases with an increase in the concentration of the sample. The highest cell inhibition is 68.6% for125 µg/ml. Thus the prepared rGO/CS/Au nanocomposite attaches to the cell

body and releases ROS resulting in deformation of cell structure, DNA damage that leads to cell death [40].

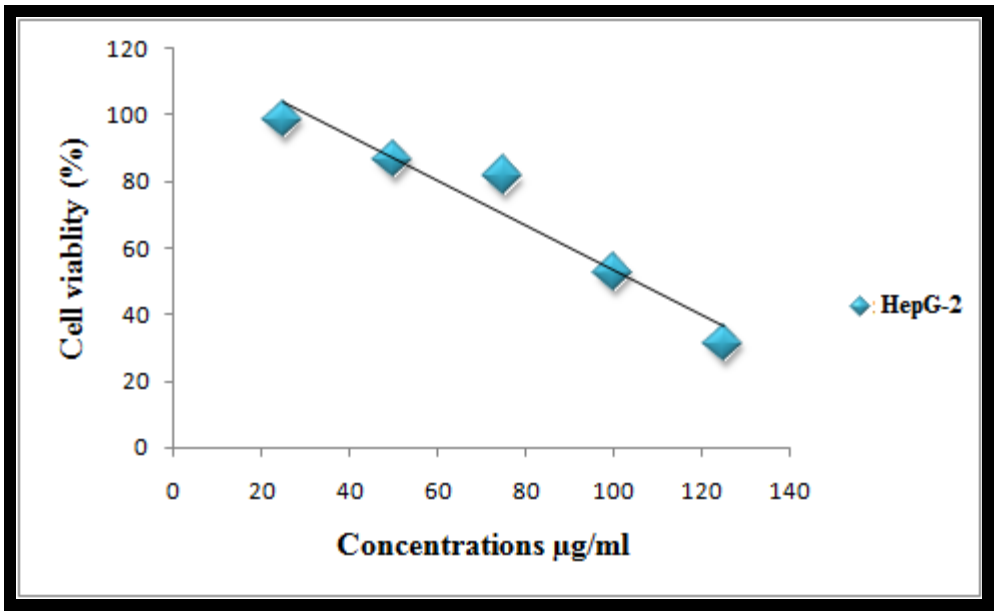

Figure 7.25 Percentage of viability versus various concentration of 0.01 M of Au nanocomposites decorated on the surface of rGO/CS nanocomposite against HepG-2 cell line

Figure 7.25 shows the cell viability curve for various concentrations (25 µg/ml, 50 µg/ml, 75 µg/ml, 100 µg/ml and 125 µg/ml) of 0.01 M of rGO/CS/Au nanocomposites against the HepG-2 cancer cell line. The percentage of cell viability is decreased to 62.5%, 52.4%, 35%, 29.8%, and 21.4% for various concentrations of 25, 50, 75, 100 and 125 µg/ml of 0.01M of rGO/CS/Au nanocomposites respectively as depicted in the Figure 7.24. The decrease in cell viability is about 21.4 % for125 µg/ml. The inhibitory concentration IC (50) of the prepared nanocomposites against HepG-2 cell line is found to be about 13.05 µg/ml. Thus the prepared nanocomposites show excellent anti proliferative activity against HepG-2 cell line.

7.9 CONCLUSION

In this chapter, the prepared rGO/CS/ZnO, rGO/CS/CuO, rGO/CS/Ag and rGO/CS/Au nanocomposites are tested for antibacterial and anticancer activity. The prepared nanocomposites show excellent bactericidal activity against both gram

positive and gram negative bacteria. The difference in bactericidal activity is due to difference in cell structure. Thus due to high release of ROS from ZnO, rGO/CS/ZnO nanocomposites shows excellent bactericidal activity compared to rGO/CS/CuO, rGO/CS/Ag and rGO/CS/Au. The synthesized nanocomposites show potent antiproliferative activity against HepG-2 cell line. The rGO/CS/Ag nanocomposites show high cytotoxicity against HepG-2 cell line compared to the rGO/CS/CuO, rGO/CS/Au and rGO/CS/ZnO nanocomposites since silver ions induces high release of ROS. These results indicate that the prepared rGO/CS/Au nanocomposites can be applied for cancer therapy due to its high antiproliferative activity.

REFERENCES

1. Anandhavelu Sanmugam, Dhanasekaran Vikraman, Hui Joon Park and Hyun-Seok Kim, Nanomaterials, One-Pot Facile Methodology to Synthesize Chitosan-ZnO-Graphene Oxide Hybrid Composites for Better Dye Adsorption and Antibacterial Activity, doi:10.3390/nano7110363, (2017).

2. Dasan Mary Jaya Seema, Bullo Saifullah, Mariadoss Selvanayagam, Sivapragasam Gothai, Mohd Zobir Hussein, Suresh Kumar Subbiah, Norhaizan Mohd Esa and Palanisamy Arulselvan, Designing of the Anticancer Nanocomposite with Sustained Release Properties by Using Graphene Oxide Nanocarrier with Phenethyl Isothiocyanate as Anticancer Agent, Pharmaceutics, doi:10.3390/pharmaceutics10030109. **(2018**).

3. Haiwei Ji, Hanjun Suna and Xiaogang Qu, Antibacterial applications of graphene-based nanomaterials: Recent review, Advanced Drug Delivery Reviews, http://dx.doi.org/10.1016/j.addr.2016.04.009.

4. Paulchamy, Arthi and Lignesh, 2015, A Simple Approach to Stepwise Synthesis of Graphene Oxide Nanomaterial, J Nanomed Nanotechnol, DOI;10.4172/2157-7439.1000253.

5. Leila shahriary and anjali a. Athawale, 2014, graphene oxide synthesized by using modified hummers approach, International journal of renewable energy and environmental engineering, ISSN: 2348-0157, vol. 02, no. 01.

6. Ahmed A. Elzatahry, Aboubakr M. Abdullah, Taher A. Salah El-Din, Abdullah M. Al-Enizi, Ahmed A. Maarouf , Ahmed Galal, Hagar K. Hassan, Ekram H. El-Ads, Salem S. Al-Theyab1 and Attiah A Al-Ghamdi, Nanocomposite Graphene-Based Material for Fuel Cell Applications , Int. J. Electrochem. Sci., 7 (2012) 3115 – 3126.

7. Hongqian Bao., Yongzheng Pan., Yuan Ping., Nanda Gopal Sahoo., Tongfei Wu., Lin Li., Jun Li and Leong Huat Gan. (2011). Chitosan-Functionalized

Graphene Oxide as a Nanocarrier for Drug and Gene Delivery. Small micro nano, DOI: 10.1002/smll.201100191.

8. Zhimin Luo., Dongliang Yang., Guangqin Qi., Lihui Yuwen., Yuqian Zhang., Lixing Weng, Lianhui Wang and Wei Huang. (2015). Preparation of Highly Dispersed Reduced Graphene Oxide Decorated with Chitosan Oligosaccharide as Electrode Material for Enhancing the Direct Electron Transfer of Escherichia coli. ACS Appl. Mater. Interfaces, 7, 8539−8544.

9. https://www.thoughtco.com/gram-positive-gram-negative-bacteria-4174239.

10. Omeed Sizar; Chandrashekhar G. Unaka, start pearls, NCBI, (2019).

11. https://www.caister.com/highveld/microbiology/gram-negative-bacteria.html

12. https://www.livescience.com/51641-bacteria.html (s aureus)

13. https://www.medicinenet.com/staph_infection/article.htm

14. David P.ClarkNanette J.Pazdernik, Chapter 1 - Basics of Biotechnology, https://doi.org/10.1016/B978-0-12-385015-7.00001-6, (2016).

15. Rivas L, Mellor G, Gobius K and Fegan N, Introduction to Pathogenic Escherichia coli. In: Detection and Typing Strategies for Pathogenic Escherichia coli. SpringerBriefs in Food, Health, and Nutrition. Springer, (2015).

16. https://about-ecoli.com/about-ecoli.

17. https://rarediseases.info.nih.gov/diseases/10085/klebsiella-infection.

18. Carol F.Farver, Bacterial Diseases, pulmonary pathology, (2016).

19. Jan Hudzicki, Kirby-Bauer Disk Diffusion Susceptibility Test Protocol, American Society for Microbiology, (2016).

20. Sandle, T. Antibiotics and preservatives. Pharmaceutical Microbiology, 171–183.doi:10.1016/b978-0-08-100022-9.00014-1, (2016).

21. Angshuman Ray Chowdhuri, Satyajit Tripathy, Soumen Chandra, Somenath Roy and Sumanta Kumar Sahu, 2015, A ZnO Decorated Chitosan-Graphene Oxide Nanocomposite Shows Significantly Enhanced Antimicrobial Activity with ROS Generation, RSC Advances, DOI: 10.1039/C5RA05393E.

22. Yan-Wen Wang, Aoneng Cao, Yu Jiang, Xin Zhang, Jia-Hui Liu, Yuanfang Liu, and Haifang Wang, Superior Antibacterial Activity of Zinc Oxide/Graphene Oxide Composites Originating from High Zinc Concentration Localized around Bacteria, doi;10.1021/am4053317.

23. Sandhya P K, Jiya Jose, M S Sreekala, M Padmanabhana, Nandakumar Kalarikkal , Sabu Thomas, 2018, Reduced graphene oxide and ZnO decorated graphene for biomedical applications, Ceramics International , https://doi.org/10.1016/j.ceramint.2018.05.143.

24. S. Archana, K.Yogesh Kumar,B.K. Jayanna, Sharon Olivera, A. Anand, M.K. Prashanth and H.B. Muralidhara, Versatile Graphene oxide decorated by star shaped Zinc oxide nanocomposites with superior adsorption capacity and antimicrobial activity, Journal of Science: Advanced Materials and Devices 3 (2018) 167e174.

25. G. Magesh, G. Bhoopathi, N. Nithya, A.P. Arun, E. Ranjith Kumar, Structural, morphological, optical and biological properties of pure ZnO and agar/zinc oxide nanocomposites, Journal of biological macromolecules, doi:10.1016/j.ijbiomac.2018.04.197.

26. Ameer Azam, Arham S Ahmed, M Oves, MS Khan and Adnan Memic, Size-dependent antimicrobial properties of CuO nanoparticles against Gram-positive and -negative bacterial strains International Journal of Nanomedicine, 7, 3527–3535, (2012).

27. Shirin Mahmood, Asghar Elmi and Somayeh Hallaj-Nezhadi, Copper Nanoparticles as Antibacterial Agents, J Mol Pharm Org Process Res, Volume 6 , Issue 1, 1000140, (2018).

28. Mohammad J. Al-Jassani and Haider Qassim Raheem, Anti-bacterial activity of CuO nanoparticles against some pathogenic bacteria, International Journal of ChemTech Research**,** 10(2), 818-822, (2017).

29. Juanni Chen, Shuyu Mao, Zhifeng Xu and Wei Ding, Various antibacterial mechanisms of biosynthesized copper oxide nanoparticles against soilborne Ralstonia solanacearum, RSC Adv, 9, 3788, (2019).

30. Haiwei Ji Hanjun Sun Xiaogang Qu , Antibacterial applications of graphene-based nanomaterials: Recent achievements and challenges, Adavanced drug delivery reviews, (2016).

31. Sadegh Khorrami, Zahra Abdollahi, Ghazaleh Eshaghi, Arezoo Khosravi, Elham Bidram and Ali Zarrabi, An Improved Method for Fabrication of Ag-GO Nanocomposite with Controlled Anti-Cancer and Anti-bacterial Behavior; A Comparative Study, scientific reports, (2019).

32. Mostafa Dadashi Firouzjaei, Ahmad Arabi Shamsabadi, Mohammad Sharifian Gh, Ahmad Rahimpour and Masoud Soroush, A Novel Nanocomposite with Superior Antibacterial Activity: A Silver-Based Metal Organic Framework Embellished with Graphene Oxide, Adv. Mater. Interfaces, 5, 1701365, (2018).

33. Feng Y, Chen, Q Yin, Q Pan, G, Tu, Z and Liu L. Reduced Graphene Oxide Functionalized with Gold Nanostar Nanocomposites for Synergistically Killing Bacteria through Intrinsic Antimicrobial Activity and Photothermal Ablation. ACS Applied Bio Materials.doi:10.1021/acsabm.8b00608, (2019).

34. Parveen Kumar, Peipei Huo, Rongzhao Zhang and Bo Liu , Antibacterial Properties of Graphene-Based Nanomaterials, Nanomaterials, 9, 737; doi:10.3390/nano9050737, (2019).

35. P. Senthilraja and K. Kathiresan, In vitro cytotoxicity MTT assay in Vero, HepG2 and MCF -7 cell lines study of Marine Yeast, Journal of Applied Pharmaceutical Science Vol. 5 (03), pp. 080-084, (2015).

36. Ashutosh Bahuguna, Imran Khan, Vivek K. Bajpai and Sun Chul Kang, MTT assay to evaluate the cytotoxic potential of a drug, Bangladesh J Pharmacol, 12,115-118, (2017).

37. Nagi El-Shafai, Mohamed E. El-Khouly Mohamed Ramadan, Ibrahim Eldesoukey and Mamdouh Masouda and Maged El-Kemary, Graphene oxide decorated with zinc oxide nanoflower, silver and titanium dioxide nanoparticles,fabrication, characterization, DNA interaction and antibacterial activity, RSC Adv, 9, 3704, (2019).

38. Arjunan Nithya, Singaravelu Chandra Mohan, Kulanthaivel Jeganathan and Kandasamy Jothivenkatachalama, A potential photocatalytic, antimicrobial and anticancer activity of chitosan copper nanocomposite, International Journal of Biological Macromolecules, 104, 1774-1782 DOI: 10.1016/j. ijbiomac.2017.03.006, (2017).

39. Thangavel Kavinkumar, Krishnamoorthy Varunkumar, Vilwanathan Ravikumar, Sellaperumal Manivannan, Anticancer activity of graphene oxide-reduced graphene oxide-silver nanoparticle composites, Journal of Colloid and Interface Science, 505 1125–1133, (2017).

40. S. Rajeshkumar, Anticancer activity of eco-friendly gold nanoparticles against lung and liver cancer cells, Journal of Genetic Engineering and Biotechnology, http://dx.doi.org/10.1016/j.jgeb.2016.05.007, (2016).